Available online at www.sciencedirect.com
SCIENCE DIRECT
Journal of Molecular Catalysis A: Chemical 235 (2005) 122–129
JOURNAL OF MOLECULAR CATALYSIS A: CHEMICAL
www.elsevier.com/locate/molcata

The role of Sn in Pt–Sn/CeO_2 catalysts for the complete oxidation of ethanol

Xiaolan Tang, Baocai Zhang, Yong Li, Yide Xu, Qin Xin, Wenjie Shen *

State Key Laboratory of Catalysis, Dalian Institute of Chemical Physics, Chinese Academy of Sciences, 457 Zhongshan Road, P.O. Box 110, Dalian 116023, PR China

Received 16 November 2004; received in revised form 2 March 2005; accepted 21 March 2005

Abstract

The structural features and catalytic properties of Pt–Sn/CeO_2 catalysts prepared by modified polyol method were extensively investigated for the complete oxidation of ethanol. CO chemisorption, TPR, DTA and XPS measurements identically indicated that the electronic configuration of Pt by Sn as well as the formation of PtSn alloy were the key factors in determining the nature of the active sites. A strong Pt/Sn atomic ratio dependence of catalytic performances was observed, which was explained in terms of the changes in the surface structure of metal phases and the electronic Pt–Sn interaction.

Keywords: Pt–Sn/CeO_2; Pt–Sn alloy; Modified polyol method; Complete oxidation of ethanol

1. Introduction

Ethanol has been regarded as promising alternative fuel for vehicles due to its high energy density, less toxicity and availability in large quantities from biomass [1]. However, the undesirable partially oxidized products in complete oxidation of ethanol, such as acetaldehyde, CO and acetic ester, can lead to severe environment and health problems. As a result, the development of efficient catalysts, which can directly converting ethanol to CO_2 and H_2O at relatively low temperatures, has been receiving renewed attention [1,2].

Supported noble metal catalysts were found to be highly active for directly converting ethanol into CO_2 with less acetaldehyde formation [1–6]. For instance, 100% conversion of ethanol was achieved over Ag/$La_{0.6}Sr_{0.4}MnO_3$ catalyst at 493 K [1], and that was obtained over Pt/Al_2O_3 even at 473 K [2]. Even though, the rapid application of ethanol in energy aspects still calls for the development of more efficient catalysts to realize the total oxidation of ethanol at temperatures as low as possible. Recent studies have shown that the beneficial effects may be obtained by the addition of promoters to the supported noble metal catalysts [7–9]. For example, platinum–tin catalysts presented extremely high catalytic activities at lower temperatures in the preferential CO oxidation [7] and the oxidation of methanol [8]. Pt–Sn/C as anode catalyst also exhibited higher electro-catalytic performance than that of Pt/C catalyst due to the enhancement of the cleavage of C–C bond by the addition of Sn [10]. The role of tin is often attributed to the formation of Pt–Sn alloy, which had better catalytic properties than Pt alone [9–12], and to the presence of well-dispersed Pt particles stabilized by tin [13]. Considering the recently reported Pt/CeO_2 catalysts, which attracted much attention with quite promising catalytic activities in various reactions [15–17], it is expectable that Pt–Sn/CeO_2 may be potential catalyst for the complete oxidation of ethanol at lower temperatures.

In the present study, Pt/CeO_2 and Pt–Sn/CeO_2 catalysts with the Pt/Sn molar ratio ranging from 3:1 to 1:2 prepared by modified polyol method, were investigated for the complete oxidation of ethanol. The electronic effect of tin on platinum in Pt–Sn/CeO_2 catalysts was also explored by means of TPR, XPS, CO chemisorption and DTA measurements. The temperature for complete oxidation of ethanol to CO_2 was

* Corresponding author. Tel.: +86 411 84379085; fax: +86 411 84694447.
E-mail address: shen98@dicp.ac.cn (W. Shen).

1381-1169/$ – see front matter © 2005 Elsevier B.V. All rights reserved.
doi:10.1016/j.molcata.2005.03.018

significantly reduced to 363 K that is about 90–120 K lower than those of previously reported [1,2].

2. Experimental

2.1. Catalyst preparation

The CeO_2 support was prepared by precipitation of $Ce(NO_3)_3{\cdot}6H_2O$ aqueous solution with the addition of $NH_3{\cdot}H_2O$ solution until the pH value of the mixture was greater than 9.0 under vigorous stirring at 333 K. The precipitant was then aged in the mother liquid for 4 h, followed by filtration and washing with distilled water. The obtained solid was dried at 373 K for 10 h, and calcined at 723 K for 4 h in air.

The metal precursors, chloroplatinic acid and tin(II) chloride, was dissolved into 60 mL ethylene glycol (EG) and mixed with 3 g CeO_2 powder. The pH value of the mixture was then adjusted to 12 by the addition of 1 M NaOH solution, and maintained at 403 K for 1 h to ensure the complete reduction of Pt. The resulting solid was filtered, washed with hot distilled water until no Cl^- anion could be detected in filtrate by $AgNO_3$ solution. After drying at 373 K for 10 h, the solid was calcined at 473 K for 2 h. The Pt loading for all samples was 3% by weight, and the Pt/Sn molar ratio varied from 3:1 to 1:2.

For comparison, monometallic 3 wt.% Pt/CeO_2 and 5 wt.% Sn/CeO_2 catalysts were prepared in the same way.

2.2. Characterization

The specific surface areas (S_{BET}) of the catalysts were calculated from a multipoint Braunauer–Emmett–Teller (BET) analysis of the nitrogen adsorption isotherms at 77 K recorded on a micrometrics ASAP 2000 instrument.

The powder X-ray diffraction (XRD) patterns were recorded using a Rigaku D/max-RB with Cu Kα radiation operated at 40 kV and 100 mA.

The CO chemisorption measurements were carried out in CHEMBET 3000 adsorption instrument (QuantaChrome Co., USA). One hundred milligrams samples were reduced in H_2 flow at 473 K for 1 h, and then purged with He at 473 K for 30 min to remove the adsorbed species. The CO chemisorption was conducted after cooling down the samples to room temperature.

The temperature-programmed reduction (TPR) measurements were conducted in a conventional setup equipped with a TCD detector. Samples of 100 mg Pt/CeO_2 or $Pt–Sn/CeO_2$ were loaded and pretreated in He flow at 473 K for 1 h to remove the adsorbed carbonates and hydrates. After cooling down to ambient temperature and introducing the reduction agent of 5% H_2/Ar, the temperature was then programmed to rise at 10 K/min.

X-ray Photoelectron Spectroscopy measurement was performed with an ESCALAB MK-II spectrometer (VG Scientific Ltd., UK) using Al Kα radiation (1486.6 eV) operated at an accelerating voltage of 12.5 kV. The powder samples were pressed into thin discs and mounted on a sample rod placed in a pretreatment chamber, in which the catalysts were reduced at desired temperatures by flowing hydrogen for 2 h. Then it was transferred into the analysis chamber where the spectra of Pt 4d, Sn 3d, Ce 3d and O 1s levels were recorded. Charging effects were corrected by adjusting the binding energy of C 1s peak to a position of 284.6 eV.

DTA experiments were performed on a Shimadzu DT-20B thermoanalysis instrument in the temperature range 300–1073 K in N_2. A temperature ramp of 10 K/min was employed.

2.3. Activity measurements

The catalytic activity tests were performed under atmospheric pressure in a continuous-flow fixed-bed reactor. Samples of 200 mg (40–60 mesh) were placed between two layers of quartz wool inside a quartz tube (i.d. = 6 mm). Prior to catalytic reactions, the catalysts were reduced with 10% H_2/He at 473 K for 2 h. The oxidation of ethanol was performed between 298 and 473 K. Liquid ethanol was injected by a micro-feeder and mixed with O_2/He mixture ($C_2H_5OH/O_2/He$ = 0.5/3/96.5 vol.%) with a gas hourly space velocity (GHSV) of 40,000 h^{-1}. Effluents from the reactor were analyzed on-line by a HP6890 gas chromatography equipped with TCD and FID detectors. A Haysep D packing column was used to detect the CO, CO_2, O_2 and H_2, and an Innowax capillary column was employed to separate oxygenates and hydrocarbons.

3. Results and discussion

3.1. Surface area and structure

The BET surface area of the CeO_2 support was measured to be 103 m^2/g, and the deposition of platinum and tin caused a significant decrease in the specific surface area. The specific surface areas of Pt/CeO_2, $Pt–Sn/CeO_2$ (Pt/Sn molar ratio = 1:1) and $Pt–Sn/CeO_2$ (Pt/Sn molar ratio = 1:2) catalysts were measured to be 92, 93 and 90 m^2/g, respectively. Fig. 1 shows the XRD patterns of CeO_2, Pt/CeO_2 and $Pt–Sn/CeO_2$ samples. As shown, the distinct fluorite oxide diffraction patterns of CeO_2 were observed in all samples, and the average crystallite size of ceria was estimated to be about 9.3 nm using the Scherrer equation. However, no diffraction peaks assigned to crystallines of platinum or tin species can be detected, even in samples after reduced at 773 K, suggesting the high dispersion of platinum and tin species on the surface of CeO_2.

Table 1 lists the CO uptakes of the catalysts. The amount of CO adsorbed on Pt/CeO_2 catalyst was measured to be 101 $\mu mol/g_{cat}$. The uptakes of CO adsorption on the bimetallic $Pt–Sn/CeO_2$ catalysts were lower than that of Pt/CeO_2 catalyst, ranging from 89 to 62 $\mu mol/g_{cat}$. This is consistent

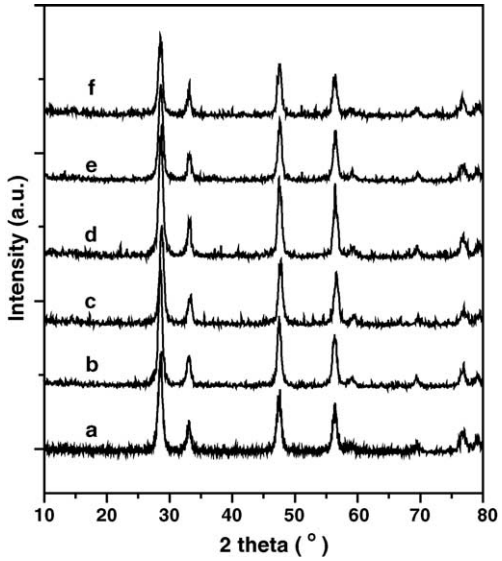

Fig. 1. XRD patterns of CeO_2, Pt/CeO_2 and $Pt–Sn/CeO_2$ catalysts: (a) CeO_2; (b) Pt/CeO_2; (c) $Pt–Sn/CeO_2$ (Pt/Sn = 1:1); (d) $Pt–Sn/CeO_2$ (Pt/Sn = 1:2); (e) $Pt–Sn/CeO_2$ (Pt/Sn = 1:1) reduced at 773 K; (f) $Pt–Sn/CeO_2$ (Pt/Sn = 1:2) reduced at 773 K.

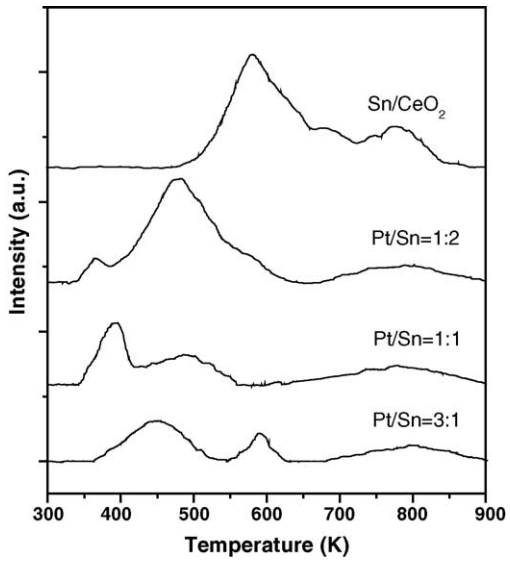

Fig. 2. TPR profiles of Sn/CeO_2 and $Pt–Sn/CeO_2$ catalysts.

with the results of Verbeek and Sachtler [17], who observed the drastic decrease in the capacity of CO adsorption over Pt–Sn systems when the Sn/Pt atomic ratio increased from 0 to 2.0. However, it should be noted that the measured CO uptakes are relative values because CO can be adsorbed on the ceria surface, especially in the presence of metals [14]. In a comparative way, the results of CO adsorption still qualitatively indicated the change of accessibility of Pt to CO with the increase of tin content.

3.2. Temperature-programmed reduction

In our previous study, the Pt/CeO_2 was found to display a single reduction peak of PtO at 244 K and reduction peak of surface CeO_2 at 670 K [16]. The TPR profiles of Sn/CeO_2 and $Pt–Sn/CeO_2$ catalysts are presented in Fig. 2. Sn/CeO_2 presented three reduction peaks at 576, 680 and 778 K. The two overlapped reduction peaks at 576 and 680 K can be ascribed to the reduction of SnO_2 to SnO_x ($1 < x < 2$) and removal of surface oxygen in CeO_2, and the peak at 778 K can be assigned to the surface reduction of SnO_x to Sn [19]. For the $Pt–Sn/CeO_2$ samples, their TPR profiles remarkably depended on the loading of tin, suggesting the presence of interaction between the two metals. The two separated reduction peaks appeared at 450 K and 595 K when the molar ratio of Pt/Sn was 3:1, respectively. The former can be assigned to the reduction of platinum oxide and the reduction of SnO_2 to SnO_x in intimate contact with platinum, and the later might be associated with the reduction of SnO_x to Sn^0. When the Pt/Sn ratio arrived at 1:1, the reduction peaks shifted to 390 and 490 K corresponding to the reductions of platinum and tin oxides, respectively. Considering the disappearance of reduction peak at 576 and 680 K, which appeared in Sn/CeO_2, it is reasonable to say that the presence of platinum induced the reduction of SnO_x by hydrogen spillover, and thus promoted the reduction of tin oxide. On the other hand, comparing with Pt/CeO_2 sample, the reduction peak of Pt oxide in $Pt–Sn/CeO_2$ shifted to higher temperature, indicating that the reduction of platinum was depressed by the addition of tin. With respect to the case of Pt/Sn = 1:2, two overlapped reduction peaks were observed at 365 and 476 K, but the intensity of low temperature reduction peak decreased accompanying by an increase in the intensity of the high temperature peak. Thus, it can be concluded the reduction of tin in Pt–Sn bimetallic catalysts depends on the Pt/Sn molar ratio, and the reduction of platinum and tin species was preceded in a synergistic way.

Table 1
CO chemisorption on Pt/CeO_2 and $Pt–Sn/CeO_2$ catalysts

Sample	CO uptake ($\mu mol/g_{cat}$)
Pt/CeO_2	101
$Pt–Sn/CeO_2$ (Pt/Sn = 3:1)	89
$Pt–Sn/CeO_2$ (Pt/Sn = 1:1)	81
$Pt–Sn/CeO_2$ (Pt/Sn = 1:2)	62

3.3. X-ray photoelectron spectroscopy

Fig. 3 compares the X-ray photoelectron spectra of Pt 4f in $Pt–Sn/CeO_2$ catalysts (Pt/Sn = 1:1 and 1:2) experienced reduction with hydrogen. The binding energies and the relative concentrations of platinum and tin species are summarized in Table 2. The XPS spectra of Pt 4f were resolved into three sets of spin-orbit doublets, which can be assigned to Pt^0, Pt^{2+} and Pt^{4+}, respectively. For the as-prepared $Pt–Sn/CeO_2$ (Pt/Sn = 1:1), Pt species presented as Pt^{2+} (46%), Pt^{4+} (15%) and Pt^0 (38%). After reduction with hydrogen at RT and 473 K, the percentages of Pt^0

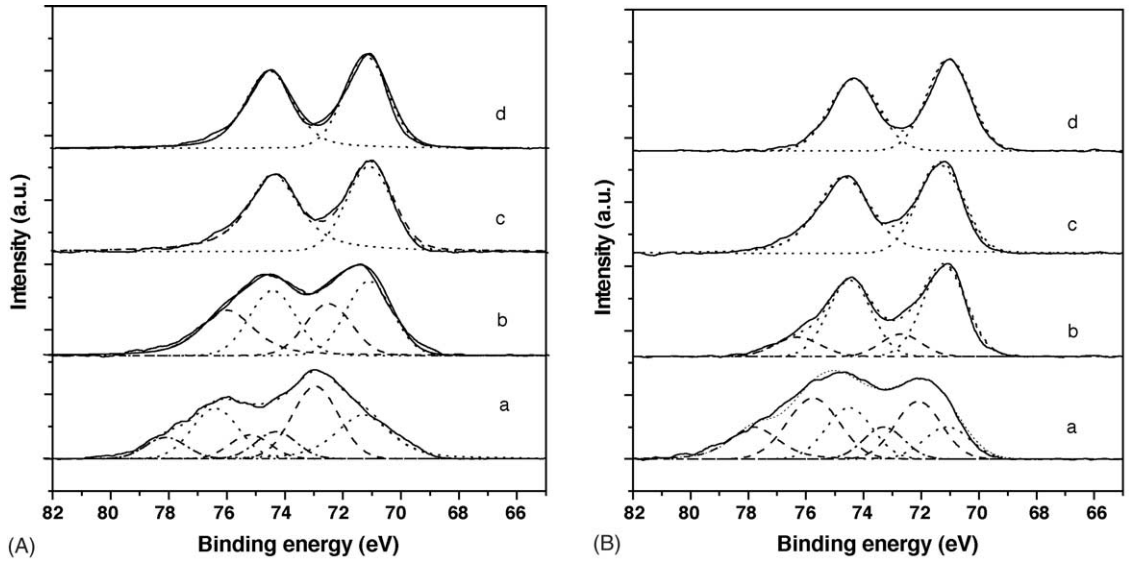

Fig. 3. (A) XPS spectra of Pt 4f for Pt–Sn/CeO_2 (Pt/Sn = 1:1): (a) as-prepared sample, and reduced with hydrogen at (b) RT, (c) 473 K, (d) 773 K; (B) XPS spectra of Pt 4f for Pt–Sn/CeO_2 (Pt/Sn = 1:2): (a) as-prepared sample, and reduced with hydrogen at (b) RT, (c) 473 K, (d) 773 K.

greatly increased to 53% and 100%. The majority of the Pt species over the as-prepared Pt–Sn/CeO_2 (Pt/Sn = 1:2) also was oxidized platinum species, and the percentages of Pt^{2+} and Pt^{4+} were 49% and 24%. Once reduced at RT, the proportion of reduced Pt species sharply increased to 81%, and the Pt species were completely reduced to Pt^0 after reduction at 473 K. Compared with the monometallic Pt/CeO_2 catalyst in which 94% of Pt^0 was presented even

Table 2
Reduction temperature dependence of component chemical states

Catalyst	Reduction temperature (K)	Platinum species	Binding energy of Pt $4f_{7/2}$ (eV)	Tin species	Binding energy of Sn $3d_{5/2}$ (eV)
Pt/CeO_2					
	Fresh	Pt^0 (54)[a]	71.5	–	–
		Pt^{2+} (31)	73.1	–	–
		Pt^{4+} (15)	74.6	–	–
	RT	Pt^0 (94)	71.6	–	–
		Pt^{2+} (6)	73.3	–	–
	473	Pt^0 (100)	71.6	–	–
	773	Pt^0 (100)	71.5	–	–
Pt–Sn/CeO_2 (Pt/Sn = 1:1)					
	Fresh	Pt^0 (39)	71.2	Sn^0 (22)[b]	485.6
		Pt^{2+} (46)	73.0	Sn^{2+}, Sn^{4+} (78)	486.8
		Pt^{4+} (15)	74.3	–	–
	RT	Pt^0 (53)	71.1	Sn^0 (28)	485.7
		Pt^{2+} (47)	72.8	Sn^{2+}, Sn^{4+} (72)	486.9
	473	Pt^0 (100)	71.1	Sn^0 (49)	485.9
				Sn^{2+}, Sn^{4+} (51)	486.8
	773	Pt^0 (100)	71.2	Sn^0 (68)	485.8
				Sn^{2+}, Sn^{4+} (32)	487.1
Pt–Sn/CeO_2 (Pt/Sn = 1:2)					
	Fresh	Pt^0 (27)	71.2	Sn^0 (20)	485.6
		Pt^{2+} (49)	72.7	Sn^{2+}, Sn^{4+} (80)	487.0
		Pt^{4+} (23)	73.6	–	–
	RT	Pt^0 (81)	71.2	Sn^0 (24)	485.9
		Pt^{2+} (19)	72.8	Sn^{2+}, Sn^{4+} (76)	486.9
	473	Pt^0 (100)	71.3	Sn^0 (56)	485.7
				Sn^{2+}, Sn^{4+} (44)	486.7
	773	Pt^0 (100)	71.2	Sn^0 (71)	485.7
				Sn^{2+}, Sn^{4+} (29)	486.8

[a] The numbers within the parentheses is referred to the content of Pt species.
[b] The numbers within the parentheses is referred to the content of Sn species.

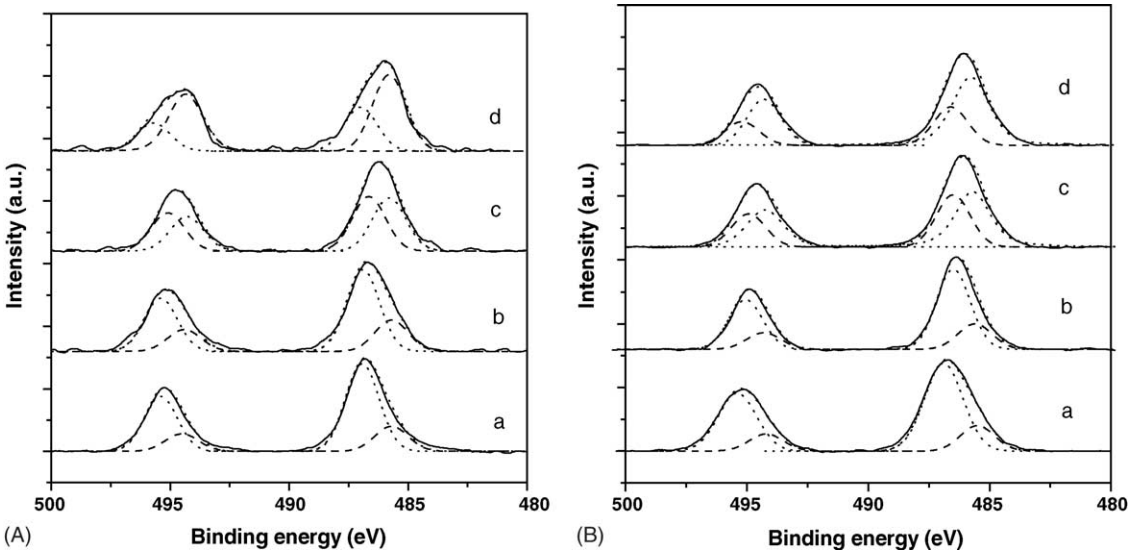

Fig. 4. (A) XPS spectra of Sn 3d for Pt–Sn/CeO_2 (Pt/Sn = 1:1): (a) as-prepared sample, and reduced with hydrogen at (b) RT, (c) 473 K, (d) 773 K; (B) XPS spectra of Sn 3d for Pt–Sn/CeO_2 (Pt/Sn = 1:2): (a) as-prepared sample, and reduced with hydrogen at (b) RT, (c) 473 K, (d) 773 K.

after reduction at RT, whereas only 50 – 80% of Pt^0 was obtained in the Pt–Sn/CeO_2 catalysts after reduction at RT, suggesting that tin suppress the reduction of Pt species. On the other hand, the binding energy of Pt $4f_{7/2}$ in Pt–Sn/CeO_2 catalysts slightly shifted towards lower values (∼0.3 eV), evidencing a possible charge transfer from Sn to Pt.

XPS spectra of Sn 3d are shown in Fig. 4, which were deconvoluted into two components: one at lower BE value (485.3 – 485.8 eV) corresponds to Sn^0 and the other at higher BE (468.6 – 487.0 eV) represents oxidized tin species. As shown in Table 2, Pt–Sn/CeO_2 catalysts showed that the percentage of Sn^0 gradually increased with the reduction temperature. Reduction at 473 K, the percentages of Sn^0 in Pt–Sn/CeO_2 (Pt/Sn = 1:1) and Pt–Sn/CeO_2 (Pt/Sn = 1:2) increased to 49% and 56%, whereas the corresponding values further increased to 68% and 71% after reduction at 773 K, respectively. This finding proved that about 70% of surface tin oxides were reduced simultaneously with platinum at temperatures below 773 K. The increase in the metallic Sn concentration also evidenced the possibility of PtSn alloys formation. Together with the downshift of the binding energy of Pt $4f_{7/2}$, as shown in Fig. 4, the binding energy of Sn $3d_{5/2}$ in Pt–Sn/CeO_2 catalysts shifted towards higher value, indicating possible electronic modification of tin through the Pt–Sn interaction.

The relative surface compositions of Pt, Sn, Ce and O elements also changed after the samples were reduced with hydrogen, as shown in Table 3. For the as-prepared Pt–Sn/CeO_2 (Pt/Sn = 1:1), the Pt/Ce and Pt/Sn ratios were 0.43 and 0.99, respectively. Reduction at RT led to obvious increase of Pt/Ce and Pt/Sn ratios. When the reduction temperature increased from RT to 773 K, the atomic ratios of Pt/Ce and Pt/Sn decreased, indicating the highly possible sintering of Pt particle, especially at higher reduction temperatures. Meanwhile, the coverage of ceria (or partially reduced ceria) on platinum surface and the simultaneously migration of tin to the surface which is often observed in CeO_2-supported metal catalysts may be another reason [20]. With regard to the Pt–Sn/CeO_2 (Pt/Sn = 1:2), the Pt/Sn molar ratio also increased initially, and then significantly decreased with the reduction temperature until it is close to the bulk Pt/Sn ratio. This behavior can be understood by considering Pt sintering and the migration of Sn from bulk to surface at reductive atmosphere. Consequently, exposed Pt surface atoms decreased with increasing tin loading and reduction temperature, suggesting some Pt particles were covered with Sn domains, especially in tin-rich sample.

Recent studies concerning Pt–Sn bimetallic system has been focused on the oxidation state of tin and the possibility of alloy formation [21,22]. In our study, XPS measurements

Table 3
Reduction temperature dependence of Pt and Sn surface compositions

Catalyst	Reduction temperature (K)	Atomic ratio		
		Pt/Ce	Pt:Sn	Ce/O
Pt/CeO_2				
	Fresh	0.74	–	0.99
	RT	0.43	–	2.28
	473	0.25	–	3.27
	773	0.58	–	2.49
Pt-Sn/CeO_2 (Pt/Sn = 1:1)				
	Fresh	0.43	0.99	1.11
	RT	0.93	1.32	0.86
	473	0.75	1.07	1.14
	773	0.52	0.94	1.23
Pt–Sn/CeO_2 (Pt/Sn = 1:2)				
	Fresh	0.50	0.83	1.10
	RT	0.61	1.26	1.03
	473	0.52	0.71	1.68
	773	0.35	0.51	1.79

clearly indicated the presence of metallic tin in both the as-prepared and the reduced Pt–Sn/CeO_2 catalysts, and the proportion of reduced tin increased with tin loading and reduction temperature. After reduction at 773 K, the proportion of Sn^0 in Pt–Sn/CeO_2 (Pt/Sn = 1:1) and Pt–Sn/CeO_2 (Pt/Sn = 1:2) increased to 68% and 71%, respectively, together with the fully reduced Pt. Thus, the alloying between tin and platinum is quite favorable under these conditions.

Additionally, the DTA measurements of the Pt-Sn/CeO_2 catalysts (Fig. 5) confirmed the occurrence of PtSn alloy with endothermal peaks emerged at 489 K for Pt–Sn/CeO_2 (Pt/Sn = 1:1) and 493 K for Pt–Sn/CeO_2 (Pt/Sn = 1:2). Similar conclusions were reached by Schubert, who confirmed that a significant fraction of the Sn in a supported PtSn catalyst involved in PtSn alloy formation after reduction in H_2, while the remaining fraction was left as unreduced tin oxides [7]. XPS and Mössbauer spectroscopy also observed that from 30% to 70% of Sn^0 presented in the form of PtSn alloy in Pt–Sn/Al_2O_3 and Pt–Sn/SiO_2 [22,23]. These results suggested the presence of a strong and effective interaction between platinum and tin in the case of bimetallic PtSn catalysts. According to above discussion, the presence of metallic tin could be explained by the formation of Pt–Sn alloy.

On the other hand, the downward shift of binding energy of platinum together with the upward shift of binding energy of tin evidenced the presence of a possible charge transfer from Sn to Pt. Moreover, the lower capacity of CO chemisorption in the bimetallic catalysts comparing to that of the monometallic one can also be related to modifications in the structure of the metallic phase that hinders the availability of surface Pt atoms to CO.

Several controversial views concerning the exact nature of Pt–Sn interaction were proposed, probably due to different preparation techniques and treatment conditions [11–24]. The way that Sn modifies the catalytic behavior of Pt can vary from bulk alloying or surface decoration to electronic interaction. Humblot et al. observed that there exist many platinum crystals surrounded mostly by tin atoms supported on SiO_2, forming so-called "sites isolation platinum crystals" [24]. The proportion of reduced tin species is close to 50%, higher than those usually reported for Pt–Sn and Rh–Sn catalysts prepared by conventional impregnation methods [25].

3.4. Activity test

The conversion of ethanol over Pt/CeO_2 and Pt–Sn/CeO_2 catalysts as a function of temperature is presented in Fig. 6. Sn/CeO_2 exhibited very low activity, no apparent ethanol conversion can be observed even at 400 K, whereas the corresponding conversion of ethanol reached 100% over Pt/CeO_2 even at 393 K. For Pt–Sn/CeO_2 catalysts, the conversion of ethanol increased initially with the addition of Sn, and approached a maximum at Pt/Sn atomic ratio of 1:1. The complete conversion temperature of ethanol over Pt–Sn/CeO_2 (Pt/Sn = 1:1) decreased to at temperature as low as 363 K. However, the conversion of ethanol decreased when the Pt/Sn atomic ratio was 1:2, even lower than that of monometallic Pt/CeO_2 catalyst. For clarity, the calculated TOF was roughly compared. It is obvious that the TOF depended on the Pt/Sn ratio. For instance, the TOF value was $4.81 \times 10^{-2}\,s^{-1}$ for the Pt–Sn/CeO_2 (Pt/Sn = 1:1) and $4.19 \times 10^{-2}\,s^{-1}$ for the Pt–Sn/CeO_2 (Pt/Sn = 3:1) at 353 K, while for Pt/CeO_2 and Pt–Sn/CeO_2 (Pt/Sn = 1:2), the corresponding values decreased to 2.01×10^{-2} and $2.42 \times 10^{-2}\,s^{-1}$, respectively. The same activity of the Pt–Sn/CeO_2 (Pt/Sn = 1:1) at 353 K was attained only at 373 K by the Pt/CeO_2 and Pt–Sn/CeO_2 (Pt/Sn = 1:2).

Acetaldehyde was the main by-product in the process of ethanol oxidation, and the amounts of ethyl acetate and methane were relatively small. Acetaldehyde and ethyl acetate were observed at low conversion levels of ethanol, while trace amounts of methane only appeared at relatively high conversions of ethanol. Figs. 7 and 8 show the temperature dependences of acetaldehyde and CO_2 selectivities over the catalysts investigated. The CO_2 selectivity increased gradually with the reaction

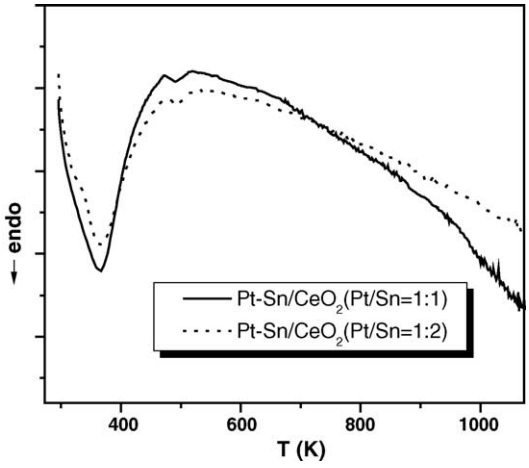

Fig. 5. DTA curves of Pt–Sn/CeO_2 catalysts.

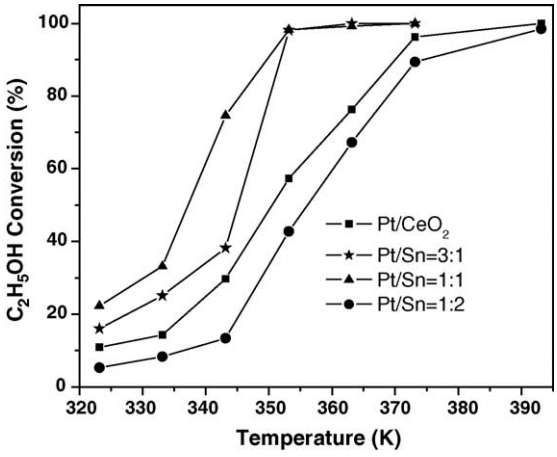

Fig. 6. C_2H_5OH conversion on Pt/CeO_2 and Pt–Sn/CeO_2 catalysts.

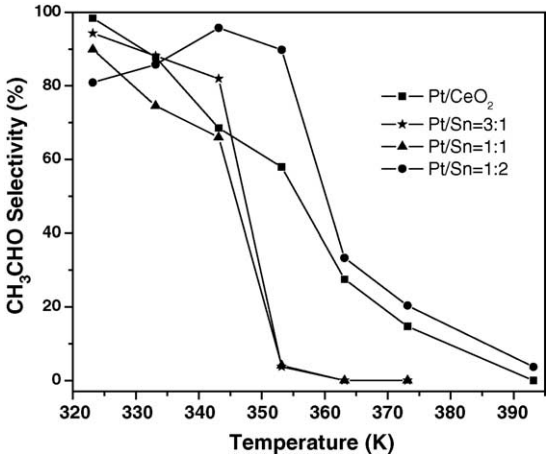

Fig. 7. Acetaldehyde selectivity over Pt/CeO_2 and $Pt–Sn/CeO_2$ catalysts.

temperature, whereas acetaldehyde selectivity presented different tendency. For $Pt–Sn/CeO_2$ (Pt/Sn = 1:1, 3:1) and Pt/CeO_2 catalysts, acetaldehyde selectivity decreased with the temperature. Whereas, for $Pt–Sn/CeO_2$ (Pt/Sn = 1:2), acetaldehyde selectivity initially increased and then dropped with reaction temperature after passing a maximum at 343 K. The relatively low acetaldehyde selectivity below 343 K was due to the formation of ethyl acetate, suggesting that addition of tin increases the selectivity of ethyl acetate at low conversion levels of ethanol. Over $Pt–Sn/CeO_2$ (Pt/Sn = 1:1) and $Pt–Sn/CeO_2$ (Pt/Sn = 3:1) catalysts, acetaldehyde selectivity reached to zero and CO_2 became the unique reaction product at 363 K. Comparatively, CO_2 became the unique product above 393 K over Pt/CeO_2 and $Pt–Sn/CeO_2$ (Pt/Sn = 1:2) catalysts. Even though, this temperature range (363 – 393 K) is still much lower than the temperatures required for the complete oxidation of ethanol to CO_2 over previous reported precious metal catalysts [1–3]. Additionally, it is needed to point out that methane appeared at different temperature domains for different samples. For $Pt–Sn/CeO_2$ (Pt/Sn = 1:1, 3:1) samples, methane occurred at the temperature range

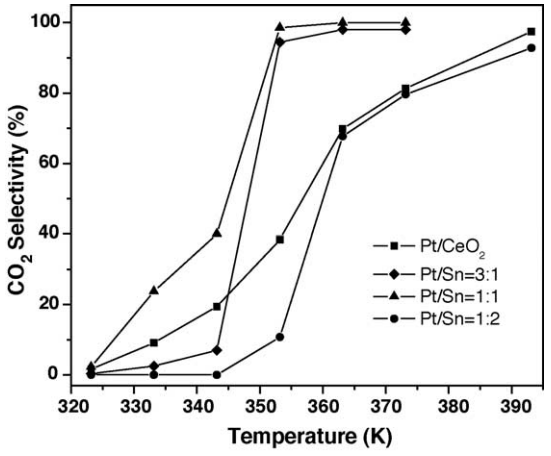

Fig. 8. CO_2 selectivity over Pt/CeO_2 and $Pt–Sn/CeO_2$ catalysts.

of 333 – 353 K, while it only was observed between 353 and 373 K over the $Pt–Sn/CeO_2$ (Pt/Sn = 1:2) and Pt/CeO_2. Considering the formation of methane must involve the leakage of C–C bond, so above discrepancy might be caused by the difference of the ability in activating C–C bond. Thus, it can be concluded that the presence of appropriate Sn can facilitate the leakage of C–C bond to form methane and CO, and then these products are further oxidized to final oxidation products. So, the ability in activating C–C bond also is an important factor in improving the catalytic performances of ethanol oxidation. Clearly, the addition of tin can promotes the catalytic performances of Pt/CeO_2 for ethanol oxidation. The $Pt–Sn/CeO_2$ (Pt/Sn = 1:1) gave the highest catalytic performances with the complete oxidation of ethanol to CO_2 and H_2O at 363 K, while higher temperatures were needed for the $Pt–Sn/CeO_2$ (Pt/Sn = 1:2) and Pt/CeO_2 catalysts.

Combining the reaction data of the complete oxidation of ethanol with the structural features of the $Pt–Sn/CeO_2$ catalysts, it is reasonable to say that the enhanced catalytic activity is associated with the modification of electronic configuration of Pt and the formation of PtSn alloy stem from the effective interaction between Pt and Sn. The charge transfer from Sn to Pt would contribute greatly to polarize the C–O and C–C bonds, and therefore favor the reaction of activated ethoxy molecules with activated oxygen species. In addition, the interaction between Pt and Sn provides different sites in close proximity of each other, Pt particles facilitate the dissociative adsorption of ethanol and Sn sites intimately adjacent to the Pt particles would provide an alternative site for O_2 activation. Consequently, this effective interaction could improve catalytic activities for ethanol oxidation. On the other hand, the separate SnO_x phase would cover active Pt sites and impede ethanol chemisorption, so higher Sn loading would lead to the decrease of the catalytic performances.

4. Conclusions

The $Pt–Sn/CeO_2$ catalysts showed considerably high catalytic performances for the complete oxidation of ethanol to CO_2 at 363 K. The modification of electronic configuration of Pt and the formation of PtSn alloys determined the nature of the active sites contributing to the increase of catalytic performances for the complete oxidation of ethanol. The separate SnO_2 phase at high tin loading would cover active Pt sites and impede ethanol chemisorption, resulting in a significant increase in the temperature required for complete oxidation of ethanol to CO_2.

References

[1] W. Wang, H.B. Zhang, G.D. Lin, Z.T. Xiong, Appl. Catal. B 24 (2000) 219.
[2] A. Marques da Silva, G. Corro, P. Marecot, J. Barbier, Stud. Surf. Sci. Catal. 116 (1998) 93.
[3] R.D. Gonzalez, M. Nagaia, Appl. Catal. 18 (1985) 57.

[4] A. Yee, S.J. Morrison, H. Idriss, Catal. Today 63 (2000) 327.
[5] P.-Y. Sheng, G.A. Bowmaker, H. Idriss, Appl. Catal. A 261 (2004) 171.
[6] C. Lamy, A. Lima, V. LeRhun, F. Delime, C. Coutanceau, J.M. Léger, J. Power Sources 105 (2002) 283.
[7] M.M. Schubert, M.J. Kahlich, G. Feldmeyer, M.S. Hackenberg, H.A. Gasteigern, R.J. Behm, Phys. Chem. Chem. Phys. 3 (2001) 1123.
[8] P. Chantarvitoon, S. Chavadej, J. Schwank, Chem. Eng. J. 97 (2004) 161.
[9] A. Erhan Aksoylu, N. Madalena, A. Freitas, J.L. Figueiredo, Catal. Today 62 (2000) 337.
[10] W.J. Zhou, Z.H. Zhou, S.Q. Song, W.Z. Li, G.Q. Sun, P. Tsiakaras, Q. Xin, Appl. Catal. B 46 (2003) 273.
[11] S.R. de Miguel, M.C. Román-Martínez, D. Cazorla-Amorós, E.L. Jablonski, O.A. Scelza, Catal. Today 66 (2001) 289.
[12] S.A. Bocanegra, A. Guerrero-Ruiz, S.R. de Miguel, O.A. Scelza, Appl. Catal. A 277 (2004) 11.
[13] R.D. Cortright, J.A. Dumesic, J. Catal. 157 (1995) 576.
[14] P. Bera, A. Gayen, M.S. Hedge, N.P. Lalla, L. Spadaro, F. Frusteri, F. Arena, J. Phys. Chem. B 107 (2003) 6122.
[15] S. Bernal, J.J. Calvino, M.A. Cauqui, J.M. Gatica, C. Larese, J.A. Pérez Omil, J.M. Pintado, Catal. Today 50 (1999) 175.
[16] X.L. Tang, B.C. Zhang, Y. Li, Y.D. Xu, Q. Xin, W.J. Shen, Catal. Lett. 97 (2004) 163.
[17] H. Verbeek, W.M.H. Sachtler, J. Catal. 42 (1976) 257.
[18] V. Perrichon, L. Retailleau, P. Bazin, M. Daturi, J.C. Lavalley, Appl. Catal. A 260 (2004) 1.
[19] M. del, C. Aguirre, P. Reyes, M. Oportus, I. Melián-Cabrera, J.L.G. Fierro, Appl. Catal. A 233 (2002) 183.
[20] A. Trovarelli, Catal. Rev. Sci. Eng. 38 (1996) 439.
[21] O.A. Barias, A. Holmen, E.A. Blekkan, Catal. Today 24 (1995) 361.
[22] Y.X. Li, K.J. Klabunde, B.H. Davis, J. Catal. 128 (1991) 1.
[23] Y.X. Li, J.M. Stencel, B.H. Davis, Appl Catal. 64 (1990) 71.
[24] F. Humblot, B. Didillon, F. LePeltier, J.P. Candy, J. Corker, O. Clause, F. Bayard, M. Basset, J. Am. Chem. Soc. 120 (1998) 137.
[25] C. Kappenstein, M. Guérin, K. Lázár, K. Matusek, Z. Paál, J. Chem. Soc., Faraday Trans. 94 (1998) 2463.